Latin American Journal of Solids and Structures
www.lajss.org

Modeling the pull-in instability of the CNT-based probe/actuator under the Coulomb force and the van der Waals attraction

Abstract
Carbon nano-tube (CNT) is applied to fabricate nano-probes, nano-switches, nano-sensors and nano- actuators. In this paper, a continuum model is employed to obtain the nonlinear constitutive equation and pull-in instability of CNT-based probe/actuators, which includes the effect of electrostatic interaction and intermolecular van der Waals (vdW) forces. The modified Adomian decomposition (MAD) method is applied to solve the nonlinear governing equation of the CNT-based actuator. Furthermore a simple and useful lumped parameter model was developed to investigate trends for various pull-in parameters. The influence of the vdW force and the geometrical dimensionless parameter on the pull-in deflection and voltage of the system is investigated. The obtained results are compared with those available in the literature as well as numerical solutions. The results demonstrate that our developed continuum based model is in good agreement with experimental results.

Keywords
Carbon nanotube probe/actuator, pull-in instability, modified Adomian decomposition (MAD), Numerical solution, Lumped parameter model

Ali Koochi[a]
Norodin Fazli[b]
Randolph Rach[c]
Mohamadreza Abadyan[a*]

[a] Shahrekord Branch, Islamic Azad University, Shahrekord, Iran.
[b] Shahrekord University of Medical Sciences, Shahrekord, Iran
[c] 316 South Maple Street, Hartford, Michigan 49057-1225, U.S.A.

[*]Corresponding Author Email: Abadyan@yahoo.com

1 INTRODUCTION

With the recent growth in nanotechnology, carbon nano-tubes (CNTs) are increasingly used in developing atomic force microscope (AFM) probes (Akita, 2001; Liet al., 2008; Cao et al., 2005), nanotweezers (Kim and Lieber, 1999) and nano-electromechanical system (NEMS) switches/actuators(Paradise and Goswami, 2007; Baughman et al., 1999; Ke et al., 2005). It has been reported that the stiffness, flexibility and strength of carbon nano-tubes are much higher than conventional materials (Esawi and Farag, 2007). Furthermore, nano-tubes can provide various ranges of conductive properties dependent on their atomic and geometrical structure (Liet al., 2008). Consider a typical cantilever CNT actuator suspended near an electrode surface with a small gap in between. Applying a voltage difference between the cantilever CNT and the conductive ground causes the CNT to deflect and be attracted toward the ground surface due to the presence of electrostatic forces. Once this voltage exceeds a critical value, an increase in the electrostatic force becomes greater than the corresponding increase in the restoring force, resulting in the unstable collapsing of the CNT to the ground position. This behavior is known as the pull-in instability and the critical voltage is called the pull-in voltage. Rasekh and Khadem (2011) studied the pull-in behavior of the cantilever CNT with nonlinearity in curvature and

inertia.When the rate of voltage variation cannot be ignored (for example in suddenly electrostatic charging), the dynamic issues i.e. the effect of inertia should be considered in the model (Lin and Zhao 2003; Moghimi Zand and Ahmadian, 2009; Sedighi, 2014). The pull-in instability related to this situation is called dynamic pull-in.

As the gap decreases from micro- to nano-scale, the van der Waals interaction predominates. The prediction of the molecular force-induced instability of CNT actuators is a critical subject in the design of AFM probes and NEMS switches/actuators(Noghrehabadi et al. 2011, 2012). With a decrease in distance between the AFM probe and the sample surface, the probe jumps onto contact with the substrate, which negates its imaging performance (Snow et al., 2002a; 2002b; Jalili and Laxminarayana, 2004, Janghorban, 2011). Wang et al. (2004) studied the influence of van der Waals attraction in the pull-in instability of frestanding nanotube based nanotweezers. They determined the critical nanotube length for each specific set of nanotube parameters by using the Galerkin method. Similarly if the minimum gap between the switch and substrate is not considered, a NEMS switch might adhere to its substrate even without an applied voltage due to the presence of intermolecular forces (Lin and Zhao, 2003, 2005a; Abadyan et al., 2010; Koochi et al., 2011a, 2011b).

In order to study nanostructures, several approaches have been employed. Molecular dynamics (MD) and molecular mechanics (MM) simulations could be used to study the mechanical behavior of carbon-based nano-materials (Desquenes et al., 2002; Tserpes, 2007; Batra andSears, 2007; Tsai and Tu, 2010). However these methods are very time-consuming and might not be easily used in modeling the performance of complex structures. An alternative reliable approach to simulate the instability behavior of a CNT interacting with an extremely large number of ground atoms is to apply an appropriate nano-scale continuum model. A hybrid continuum model can be similarly used to calculate the van der Waals energy, in lieu of the discrete Lennard-Jones potential (Desquenes et al., 2002; Batra andSears, 2007;Gupta and Batra, 2008). Although continuum models are more time-saving than the MM and MD, their approach often leads to nonlinear equations that might not be amenable by common analytical methods (Lin WH, Zhao 2005b; Desquenes et al., 2002).

In this paper, the pull-in instability of the cantilever CNT probe/actuator has been investigated. The modified Adomian decomposition (MAD) is applied to solve the nonlinear governing equation of this CNT-based system. It has been shown that MAD is a powerful and convenient method which can effectively solve a large class of highly nonlinear problems(Rach, 2012; Duan et al., 2008; Soroush, et al., 2012; Koochi et al., 2010; 2012; 2013).Moreover a lumped parameter model (LPM) is developed to simply explain trends in the physical influence of nano-scale effects on the pull-in performance of the CNT-based system. The obtained results are verified by comparing with those from the literature as well as numerical solutions.

2 Theoretical Mode

Consider a freestanding multi-walled CNT probe/actuator above a ground plane consisting of multiple graphene layers, with an interlayer distance of $d = 3.35$ Å, as illustrated in figure 1. The length of the CNT is L and the initial gap between the CNT and the ground is D. The boundary conditions of the CNT are defined as a fixed cantilever at one end with no displacement and rotation and traction free at the free end with no shear force and moment.

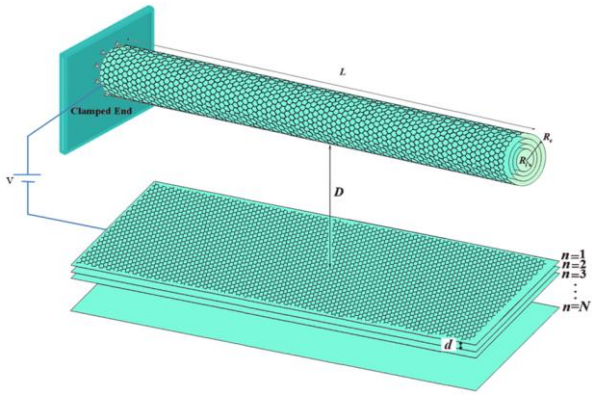

Figure 1: Schematic representation of the cantilever CNT switch/actuator.

2.1. Electrostatic interaction

When a conductive nano-tube is placed over a conductive substrate (in the presence of an applied potential difference between the tube and the electrode), the electrostatic charge is induced on both the tube and the substrate. To calculate the electrical forces acting on the tube, a capacitance model may be used. For infinitely long conductive cylinders, the capacitance per unit length is given by (Hayt and Buck, 1930):

$$C(q) = \frac{2\pi\varepsilon_0}{\operatorname{arccosh}(1+\frac{D}{R_w})} \tag{1}$$

Where D is the initial distance between the tube and ground plate, and ε_0=8.854×10^{-12} C^2/Nm^2 is the permittivity of vacuum. Therefore the electrostatic force per unit length is given by:

$$f_{elec} = \frac{d(\frac{1}{2}C(D)V^2)}{d(D)} = \frac{\pi\varepsilon_0 V^2}{\sqrt{D(D+2R_w)}\operatorname{arccosh}^2(1+\frac{D}{R_w})}, \tag{2}$$

where R_w is the radius of CNT and V isthe applied voltage.
By applying an external voltage differential, the nano-tube deflects towards the ground and the distance between the nano-tube and the ground plate reduces to D-U. By considering $D \pm R_w \approx D$, the electrostatic force per unit length of the deflected actuator can be further simplified as:

$$f_{elec} = \frac{\pi\varepsilon_0 V^2}{(D-U)\operatorname{arccosh}^2(\frac{D-U}{R_W})} = \frac{\pi\varepsilon_0 V^2}{(D-U)\ln^2(2\frac{D-U}{R_W})}, \tag{3}$$

2.2. van der Waals interactions

A reliable continuum model has been established to compute the van der Waals (vdW) energy by the double-volume integral of the Lennard-Jones potential (Lennard-Jones, 1930). This method provides acceptable results for explaining the CNT-graphene substrate attraction compared to

that of direct pair wise summation through molecular dynamics. For a single walled carbon nanotube (SWCNT) over a graphene surface and for distances larger than 5 Å, the difference between the two values of the E_{vdW}, as specified by the continuum model and molecular dynamics, is less than 1% (Tserpes, 2007). Using this approach, the energy per unit length of the carbon nano-tube is simplified as (Tserpes, 2007):

$$\frac{E_{vdW}}{L} = -C_6\sigma^2\pi^2 \sum_{R=R_i}^{R_o} \sum_{r=D}^{D+(N-1)d} \frac{R(R+r)[3R^2+2(R+r)^2]}{2[(R+r)^2-R^2]^{3.5}}, \tag{4}$$

where R_i and R_o are the inner and outer radii of the CNT, N is the number of graphene sheets and $\sigma \cong 38$ nm^{-2} is the graphene surface density. The parameter C_6 is the constant of attraction that equals 15.2 eVÅ^6 for the carbon-carbon interaction (Girifalco et al., 2000). Once the van der Waals energy is computed, the corresponding energy terms are used to derive the component of the intermolecular force per unit length, f_{vdW}, along the r-direction. In most applications, it is practical to assume that the diameter of tube is much smaller than the distance between the nanotube and the graphene surface, i.e. $(2R) << D$. According to this assumption, equation (4) is simplified as

$$\begin{aligned} f_{vdW} &= -\frac{d(\frac{E_{vdW}}{L})}{dr} = C_6\sigma^2\pi^2 \sum_{R=R_i}^{R_o} \sum_{r=D}^{D+(N-1)d} \frac{R(8r^4+32r^3R+72r^2R^2+80rR^3+35R^4)}{2r^{4.5}(r+2R)^{4.5}} \\ &\approx 4C_6\sigma^2\pi^2 N_W R_W \sum_{r=D}^{D+(N-1)d} \frac{1}{r^5}, \end{aligned} \tag{5}$$

where N_W is the number of walls of the nanotube and R_W is the mean value of their radii.
For a large number of layers, i.e. $D + (N\text{-}1)d >> D$, replacing the summation with an integral yields

$$\sum_{r=D}^{D+(N-1)d} \frac{1}{r^5} \approx \frac{1}{d}\int_D^{D+(N-1)d} \frac{1}{r^5}dr = \frac{1}{4d}[\frac{1}{D^4} - \frac{1}{(D+(N-1)d)^4}] \approx \frac{1}{4dD^4} \tag{6}$$

Lastly obtain

$$f_{vdW}(D) \approx C_6\sigma^2\pi^2 N_W R_W d^{-1}D^{-4}. \tag{7}$$

2.3. Governing equations

In order to develop the governing equation of the beam, the constitutive material of the CNT is assumed to be linear elastic, and only the static deflection of the nano-tube is considered. The minimum energy principle was applied, which implies a state of equilibrium, when the free energy reaches a minimum value. By applying the Hamilton principle, the governing equilibrium equation can be determined as:

$$\delta W = \delta W_{elas} - \delta W_{elec} - \delta W_{vdW} = \int_0^L (E_{eff} I \frac{d^2U}{dX^2} \delta \frac{d^2U}{dX^2} - f_{elec}\delta U - f_{vdW}\delta U) dX$$
$$= E_{eff} I \frac{d^2U}{dX^2} \delta \frac{dU}{dX}\Big|_0^L - E_{eff} I \frac{d^3U}{dX^3} \delta U\Big|_0^L + \int_0^L (E_{eff} I \frac{d^4U}{dX^4} - f_{elec} - f_{vdW})\delta U dX = 0, \quad (8)$$

Where δ denotes the variation symbol, X is the position along the nano-tube measured from the clamped end, U is the beam deflection, E_{eff} is the effective Young's modulus of the CNT, which is typically 0.9-1.2 TPa (Desquenes et al., 2002) and I is the cross-sectional moment of inertia, which equals $\pi(R_o^4 - R_i^4)/4$. By integrating equation (8), the governing equation of the cantilever nano-tube actuator is derived as

$$EI \frac{d^4U}{dX^4} = f_{elec} + f_{vdW}, \quad (9.a)$$

$$U(0) = \frac{dU}{dX}(0) = 0 \text{ (Geometrical B.C. at the fixed end)}, \quad (9.b)$$

$$\frac{d^2U}{dX^2}(L) = \frac{d^3U}{dX^3}(L) = 0 \text{ (Natural B.C. at the free end)}. \quad (9.c)$$

Equations (9. a-c) can be made dimensionless using the following substitutions:

$$u = \frac{U}{D},$$
$$x = \frac{X}{L},$$
$$f = \frac{C_6 \sigma^2 \pi^2 N_W L^4}{dE_{eff} I D^4},$$
$$k = \frac{D}{R_W} \text{ and}$$
$$\beta = \frac{\pi \varepsilon_0 V^2 L^4}{E_{eff} I D^2}. \quad (10)$$

These transformations yield

$$\frac{d^4u}{dx^4} = \frac{f}{k(1-u(x))^4} + \frac{\beta}{(1-u)\ln^2[2k(1-u)]}, \quad (11.a)$$

$$u(0) = \frac{du}{dX}(0) = 0 \text{ (Geometrical B.C. at the fixed end)}, \quad (11.b)$$

$$\frac{d^2u}{dx^2}(L) = \frac{d^3u}{dx^3}(L) = 0 \text{ (Natural B.C. at the free end)}. \quad (11.c)$$

3 Solution methods

3.1 The modified Adomian decomposition method

The basic idea of the modified Adomian decomposition (MAD) is explained in (Wazwaz, 2001). In order to apply the MAD, the boundary value problem is solved using a rapidly convergent infinite series. The details of the method and mathematical computations are explained in Appendix A. Briefly, the analytical MAD solution of Equation (11) can be obtained as the following formula:

$$\begin{aligned} u(x) = & -\frac{1}{2!}C_1x^2 - \frac{1}{3!}C_2x^3 + \frac{1}{4!}(\frac{f}{k} + \frac{\beta}{\ln^2(2k)})x^4 \\ & -\frac{1}{6!}(\frac{4f}{k} + \frac{\beta}{\ln^2(2k)} + \frac{2\beta}{\ln^3(2k)})C_1x^6 - \frac{1}{7!}(\frac{4f}{k} + \frac{\beta}{\ln^2(2k)} + \frac{2\beta}{\ln^3(2k)})C_2x^7 \\ & +\frac{1}{8!}\{(\frac{f}{k} + \frac{\beta}{\ln^2(2k)})(\frac{4f}{k} + \frac{\beta}{\ln^2(2k)} + \frac{2\beta}{\ln^3(2k)})C_2 + [\frac{60f}{k} + \frac{6\beta}{\ln^2(2k)}(1 + \frac{3}{\ln(2k)} + \frac{3}{\ln^2(2k)})]C_1\}x^8 \\ & +\frac{1}{9!}[\frac{200f}{k} + \frac{20\beta}{\ln^2(2k)}(1 + \frac{3}{\ln(2k)} + \frac{3}{\ln^2(2k)})]C_1C_2x^9 + ..., \end{aligned} \tag{12}$$

where the constants C_1 and C_2 can be determined by solving the resulting algebraic equation from the B.C at $x = 1$ i.e. using equation (11-b). For any given values of f, β and k, equation (12) can be used to obtain the pull-in parameters of the nano-tube actuator. The instability in equation (12) occurs when $d\beta(x=1)/du \to 0$. The pull-in voltage of the system can be determined by plotting the coordinates u vs. β.

3.2 The lumped parameter model

The lumped parameter model only simulates the tip of the cantilever. In order to develop a simple lumped parameter model (LPM), the nano actuator shown in figure 1 is replaced by a simplified one-dimensional structure; see figure 2. The structure is constructed from a linear spring with a stiffness of K. The model assumes a uniform force distribution q along the beam. The elastic stiffness of the structure of a cantilever beam is $K=8EI/L^3$, therefore the relation between the dimensionless beam tip deflection, u_{tip}, and the applied voltage, β, can be defined as:

$$\beta = 8u_{tip}(1-u_{tip})\ln^2[2k(1-u_{tip})] - \frac{f\ln^2[2k(1-u_{tip})]}{k(1-u_{tip})^3} \tag{13}$$

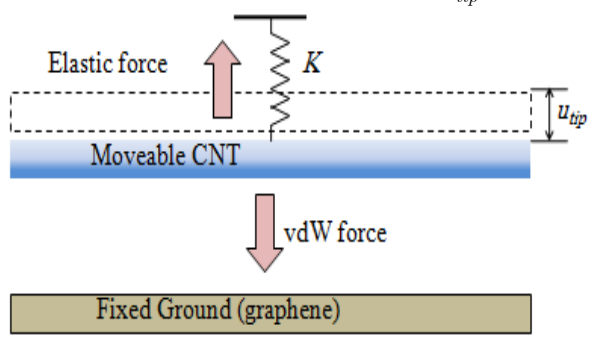

Figure 2: Schematic representation of the lumped parameter model for a cantilever switch.

3.3 Numerical solution

In order to verify the analytical results, the cantilever beam-type NEMS is numerically simulated and these results are compared with those obtained by the MAD and LPM. The nonlinear governing differential equation (11), is solved using the boundary value problem solver of the commercial MAPLE software package. The step size of the parameter variation is chosen based on the sensitivity of the parameter to the tip deflection. The pull-in parameters of the system can be determined from inspection of the slope of the u-β graphs.

4 Results and Discussion

4.1. CNT Deflection and Pull-in instability

Figure 3 shows the centerline deflection of a typical CNT probe/actuator under intermolecular force and external voltage obtained using the MAD and numerical methods. When the applied voltage increases from zero to its critical value (pull-in voltage), the CNT deflection increase from its initial value to the final stable deflection (pull-in deflection). This figure reveals a good agreement between the pull-in deflection and pull-in voltage values obtained by numerical solution and the analytical MAD. The relative error of MAD method with respect to the numerical solution is within the acceptable range for engineering applications and can be reduced by selecting more series terms.
The relations between the applied voltage and centerline tip deflection, when k=10 and k=50, are presented in figures 4 and 5, respectively. These figures show that when the applied voltage exceeds its critical value β_{PI}, no solution exists for u_{tip} and the pull-in instability occurs.

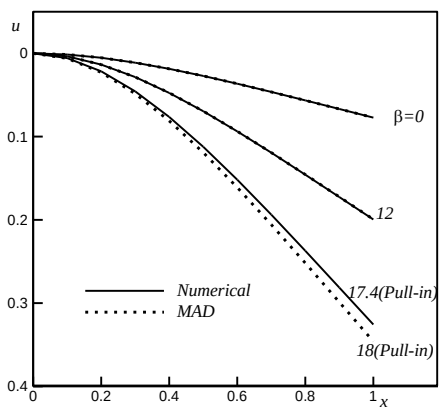

Figure 3: Deflection of thecantilever CNT fordifferentvalues of $\beta$when $f = 25$ and k= 10.

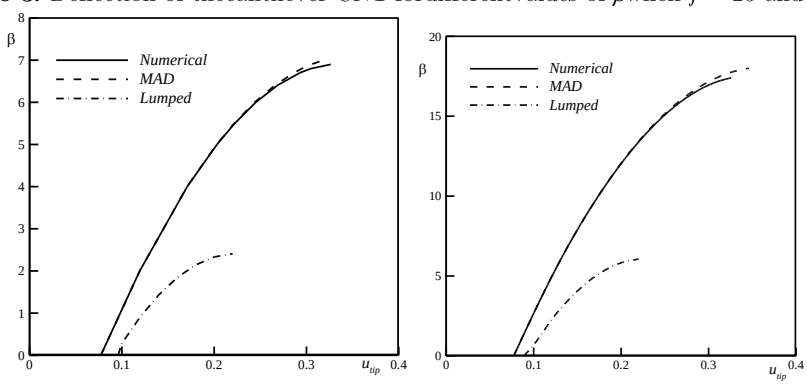

(a) (b)

Figure 4: Theparameterβ as a function of $u_{\text{tip}}$for$f/k = 0.5$ when (a) $k = 10$ (b) $k = 50$.

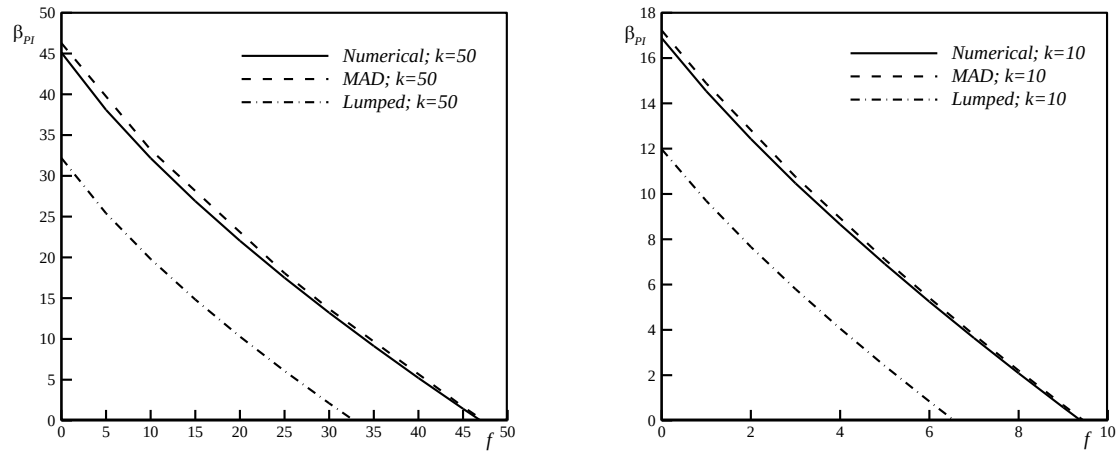

(a) (b)

Figure 5: Effect of the van der Waals force (f) onβ_{PI} (a) k=10)b) k=50

4.2. Effect of vdW force (f) on pull-in behavior

Figure 3 reveals that the CNT has an initial deflection due to the presence of the vdW attraction even without applying a voltage difference. This effect can be observed in figure 4 where the intersections of the curves with the horizontal axis correspond to the initial tip deflection of CNT induced by the presence of vdW attraction.The maximum length of the CNT, L_{max}, at which the CNT does not stick to the substrate without the application of a voltage difference is called the detachment length (Lin and Zhao, 2003; 2005a). The detachment length is the maximum permissible length of the freestanding CNT. On the other hand, if the length of CNT is known, there is a minimum gap, D_{min}, which prevents stiction due to the van der Waals forces. The L_{max} and D_{min} are very important for reliable operation of CNT probe/actuator and can be determined from the critical value of vdW force.

The effect of molecular force on pull-in voltage of the CNT probe/actuatoris presented in figure 5 for different values of k, k=10 and k=50. As shown, increasing the intermolecular force leads to a decrease in the pull-in voltage of the CNT probe. Note that the intersection point of the curves and the horizontal axis corresponds to the critical value of the molecular force. This reveals when the gap between CNT and ground is sufficiently small, the van der Waals force can induce stiction even without any electrostatic force.

Influence of vdW force on the pull-in deflection of the CNT is presented in figure 6(a) and 6(b) for k=10 and k=50, respectively. Figure 6 shows that increasing the van der Waals force reduces the pull-in deflection of the CNT.

4.3. Effect of geometrical parameter on pull-in behavior

The geometrical parameter k corresponds to the ratio of gap distance to CNT diameter. Comparison between figures 5(a) and 5(b) reveals that increasing the values of k results in increasing the pull-in voltage of CNT. This physically reveals that increasing the initial gap between CNT and ground results in increasing the instability voltage of the system. However, k parameter has no significant effect on the pull-in deflection of the system. Comparison between figures 5(a) and 6(b) reveals no substantial change in the pull-in deflection of the system due to increasing the values of k.

4.4. Comparison with experiment

In order to verify the computed values, the pull-in voltage of a typical cantilever CNT-based nano-probe with the following parameters was compared to experimental data in Table 1. The length of the nanotube is L= 6.8 μm, the initial gap between the nanotube and electrode is D = 3 μm, and the radius and modulus of CNT are R_w=5 nm and E=1 TPa, respectively. As shown, the theoretical results are in good agreement with the experimental data. Interestingly, neglecting the vdW force provides only 1 % change in the pull in voltage of the system. This shows that vdW force might be omitted in real cases. However, in the case of freestanding cases or when the initial gap is very small, vdW has a significant effect on pull-in behavior of the system.

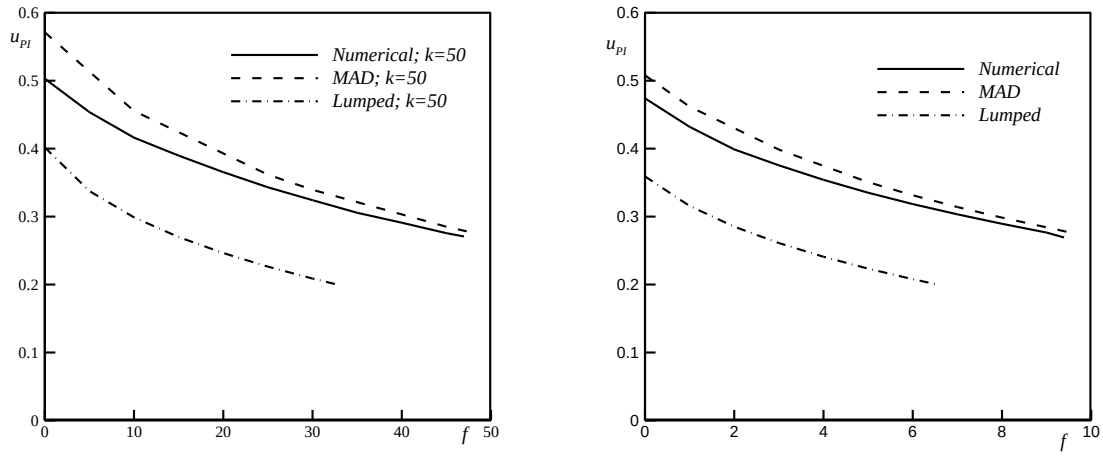

(a) (b)

Figure 6: Effect of the van der Waals force*f*onu_{PI}: (a) k = 10 b) k = 50.

Table 1. Pull-in voltage obtained from different methods

Method	Experimental (Ke et al., 2005)	MAD	Lumped	Numerical
Pull-in Voltage (volte)	48	50.39	42.03	48.79

Finally, in orderto determine the van der Waals interactionbetweendifferentmaterials (forexample CNT actuatorover a goldsubstrate), one can utilizetheHamakerconstant, A, thatisdetermined as:

$$A = \pi^2 \rho_1 \rho_2 C_6 \tag{14}$$

whereϱ_1 and ϱ_2 are thenumber of atoms per unitvolume in twointeractingbodies and C_6isthecoefficient in theparticle-particlepairinteraction (see Lee and Sigmund, 2002).

5 Conclusions

In this work, the pull-in behavior of a cantilever CNT actuator has been investigated using a nano-scale continuum model. It is observed that when the applied voltage increase to its critical value (pull-in voltage), the CNT deflection reaches to its final stable value (pull-in deflection). The presence of the vdW force reduces the pull-in deflection and voltage of the CNT probe/actuator. Moreover, when the gap between CNT and ground is sufficiently small, the vdW force can induce instability even without any electrostatic force. It is found that increasing the

initial gap to radius ratios (k) of the system increases its pull-in voltage. However, variation of k parameter has no significant effect on the pull-in deflection of the system. Results of this study reveal that the analytical MAD is a reliable method for analyzing the pull-in behavior of CNT-based probe/actuators. The MAD results are very close to the numerical solution as well as experiments in literature. While lumped parameter model is useful to simplify simulations of the physical behavior of the nanostructure for predicting trends, it cannot accurately predict the pull-in parameters of the system. The proposed continuum model avoids time-consuming molecular dynamics computations and makes parametric studies possible.

Appendix A: The Modified Adomian Decomposition Method (MAD)

In order to solve equation (11) by the MAD analytical method, consider a nonlinear differential equation of a fourth-order boundary-value problem (Wazwaz, 2001),

$$y^{4}\ x\ = f\ x,y\ , \qquad 0 \le x \le L_b, \tag{A.1}$$

With boundary conditions

$$y\ 0\ = \alpha_0, \qquad y'\ 0\ = \alpha_1 \tag{A.2}$$

Equation (A.1) can be represented as

$$L^{4}\left[y\ x\ \right] = f\ x,y \tag{A.3}$$

Where $L^{(4)}$ is a differential operator, which is defined as

$$L^{4}\ = \frac{d^{4}}{dx^{4}} \tag{A.4}$$

The corresponding inverse operator $L^{(-4)}$ is defined as a 4-fold integral operator, that is

$$L^{-4}\ = \underbrace{\int_0^x \ldots \int_0^x .\ dx \ldots dx}_{\text{4-fold}} \tag{A.5}$$

Employing the Adomin decomposition method (Nayfeh et al., 2005), the dependent variable in Equation (A.1) can be written as

$$y\ x\ = \sum_{n=0}^{\infty} y_n\ x \tag{A.6}$$

Referring to the modified Adomian decomposition method from (Nayfeh et al., 2005), the recursive relations of Equation (A.6) can be provided as

$$\begin{aligned} y_0 \;\; x \;\; &= \alpha_0 \;, \\ y_{n+1} \;\; x \;\; &= L^{-4} \left[f_k \right]. \end{aligned} \tag{A.7}$$

If *f(g)* is a nonlinear function, then the nonlinear term *N[f(g)]* can be represented as a series of Adomian polynomials tailored to the particular nonlinearity (Adomian, 1983).

$$N\Big[f \;\; g \;\Big] = \sum_{n=0}^{\infty} A_n \;, \tag{A.8}$$

where the individual $A_n$are determined from the following formula:

$$A_n = \frac{1}{n!} \frac{d^n}{d\lambda^n} \Big[f \;\; g \;\; \lambda \;\; \Big]_{\lambda=0}. \tag{A.9}$$

Referring to (Adomian, 1983; Rach, 1984), it can further be presented as the following convenient equations

$$A_n = \sum_{v=1}^{n} C(v,n) h_v(g_0), \tag{A.10}$$

Where

$$C(v,n) = \sum\nolimits_{p_i} \prod\nolimits_{i=1}^{v} \frac{1}{k!} g_{p_i}^{k_i}, \qquad \sum_{i=1}^{v} k_i p_i = n, n > 0, \;\; 0 \le i \le n, \text{ for } 1 \le p_i \le n - v + 1 \tag{A.11}$$

and k_i is the number of repetitions in the g_p, the values of p are selected from the above range by combination without repetition, $h_\nu(g_0)$ is calculated by differentiating the nonlinear terms $f(g)$, ν times with respect to g at $\lambda = 0$, and can be represented as

$$h_v(g_0) = \frac{d^v}{dg^v} [f(g(\lambda))]_{\lambda=0} \tag{A.12}$$

Hence, it is convenient to obtain the Adomian polynomials as

$$\begin{aligned} &A_0 = h_0(g_0) \\ &A_1 = C(1,1)h_1(g_0) = g_1 h_1(g_0) \\ &A_2 = C(1,2)h_1(g_0) + C(2,2)h_2(g_0) = g_2 h_1(g_0) + \frac{1}{2!} g_1^2 h_2(g_0) \\ &A_3 = C(1,3)h_1(g_0) + C(2,3)h_2(g_0) + C(3,3)h_3(g_0) = g_3 h_1(g_0) + g_1 g_2 h_2(g_0) + \frac{1}{3!} g_1^3 h_3(g_0) \\ &..... \end{aligned} \tag{A.13}$$

Substituting relations (A.12) in equation (A.13), we obtain the solution components as

$$
\begin{aligned}
&y_0 = 1\\
&y_1 = \frac{1}{2!}C_1x^2 + \frac{1}{3!}C_2x^3 - \frac{1}{4!}(\frac{f}{k} + \frac{\beta}{\ln^2(2k)})x^4\\
&y_2 = \frac{1}{6!}(\frac{4f}{k} + \frac{\beta}{\ln^2(2k)} + \frac{2\beta}{\ln^3(2k)})C_1x^6 + \frac{1}{7!}(\frac{4f}{k} + \frac{\beta}{\ln^2(2k)} + \frac{2\beta}{\ln^3(2k)})C_2x^7\\
&-\frac{1}{8!}(\frac{f}{k} + \frac{\beta}{\ln^2(2k)})(\frac{4f}{K} + \frac{\beta}{\ln^2(2k)} + \frac{2\beta}{\ln^3(2k)})C_2x^8\\
&y_3 = -\frac{1}{8!}[\frac{60f}{k} + \frac{6\beta}{\ln^2(2k)}(1 + \frac{3}{\ln(2k)} + \frac{3}{\ln^2(2k)})]C_1^2x^8 - \frac{1}{9!}[\frac{200f}{k} + \frac{20\beta}{\ln^2(2k)}(1 + \frac{3}{\ln(2k)} + \frac{3}{\ln^2(2k)})]C_1C_2x^9\\
&+\frac{1}{10!}\{60[(\frac{f}{2k} + \frac{\beta}{2\ln^2(2k)})C_1 - \frac{C_2^2}{3}][\frac{10f}{k} + \frac{\beta}{\ln^2(2k)}(1 + \frac{3}{\ln(2k)} + \frac{3}{\ln^2(2k)})] + (\frac{4f}{k} + \frac{\beta}{\ln^2(2k)} + \frac{2\beta}{\ln^3(2k)})^2\}x^{10}\\
&+\frac{1}{11!}\{70(\frac{f}{k} + \frac{\beta}{\ln^2(2k)})[\frac{10f}{K} + \frac{\beta}{\ln^2(2k)}(1 + \frac{3}{\ln(2k)} + \frac{3}{\ln^2(2k)})] + (\frac{4f}{K} + \frac{\beta}{\ln^2(2k)} + \frac{2\beta}{\ln^3(2k)})^2\}C_2x^{11}\\
&-\frac{1}{12!}\{(\frac{f}{k} + \frac{\beta}{\ln^2(2k)})(\frac{4f}{K} + \frac{\beta}{\ln^2(2k)} + \frac{2\beta}{\ln^3(2k)})^2 + 840[\frac{10f}{k} + \frac{\beta}{\ln^2(2k)}(1 + \frac{3}{\ln(2k)} + \frac{3}{\ln^2(2k)})](\frac{4f}{k} + \frac{\beta}{\ln^2(2k)} + \frac{2\beta}{\ln^3(2k)})^2\}x^{12}\\
&\cdots.
\end{aligned}
\tag{A.14}
$$

Appendix B: Considerations Concern with Pull-In Behavior

It should be noted that the pull-in instability is actually a Hopf bifurcation problem. Pull-in occurs when any perturbation from the equilibrium produces electrical force/moment that cannot be balanced with resistive elastic force/moment. When applied voltage is less than instability voltage, the stability of solution should be considered to capture stable equilibrium point. MAD solution can successfully predict not only the stable (lower) branch but also the unstable (upper) branch, as shown in figure B.1. The upper and lower branches of equilibrium converge at a saddle-like bifurcation point, where the pull-in voltage can be determined.

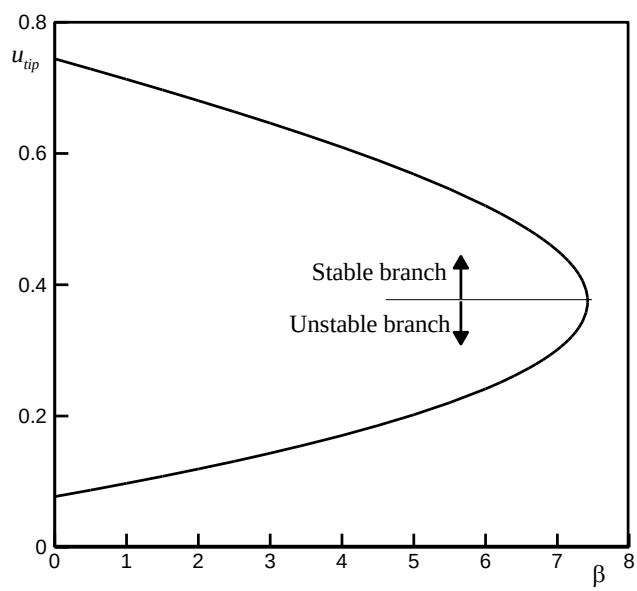

Figure B.1: The variation of tip displacement of CNT versus the applied voltage parameter for k=10 and f=5

Moreover, when the rate of voltage variation is not negligible i.e suddenly electrostatic loading, the effect of inertia should be considered. The pull-in instability related to this situation is called dynamic pull-in instability and the critical value of voltage, corresponding to the dynamic instability, is referred to as the dynamic pull-in voltage (Lin and Zhao 2003; Moghimi Zand and Ahmadian, 2009; Sedighi, 2014). In this paper we assume the rate of voltage variation is negligible but when the rate of voltage variation is not negligible, the effect of inertia should to be considered. Investigation of dynamic pull-in is beyond the scope of present work.

References

Abadyan, M., Novinzadeh, A., Kazemi, A. S. (2010). Approximating the effect of Casimir force on the instability of electrostatic nano-cantilevers. Physica Scripta 81:015891(10pp).

Adomian G. (1983). Stochastic Systems, Academic Press(London)

Akita, S. (2001). Nanotweezers consisting of carbon nanotubes operating in an atomic force microscope. Applied Physics Letters 79:1591–1593.

Batra, R. C., Sears, A. (2007). Continuum models of multi-walled carbon nanotubes. International Journal of Solids and Structures 44:7577-7596.

Baughman, R. H., Cui, C., Zakhidov, A. A., Iqbal, Z., Barisci, J. N., Spinks, G. M., Wallace G. G., Mazzoldi, A., Rossi, D. D., Rinzler, A. G., Jaschinski, O., Roth, S., Kertesz, M. (1999). Carbon nanotube actuators. Science 284:1340-1344.

Cao, Y., Liang, Y., Dong, S., Wang, Y. (2005). A multi-wall carbon nanotube (MWCNT) relocation technique for atomic force microscopy (AFM) samples. Ultramicroscopy 103(2):103-108.

Desquenes, M., Rotkin, S. V., Alaru, N. R. (2002). Calculation of Pull-in Voltages for Carbon-Nanotube-Based Nanoelectromechanical Switches. Nanotechnology 13:120-131.

Duan, J. S., Rach, R., Baleanu, D., Wazwaz, A. M. (2012). A review of the Adomian decomposition method and its applications to fractional differential equations. Communications in Fractional Calculus 3(2) 73-99.

Esawi, A. M. K., Farag, M. M. (2007). Carbon nanotube reinforced composites: Potential and current challenges. Materials & Design 28(9):2394-2401.

Girifalco, L. A., Hodak M., Lee, R. S. (2000).Carbon nanotubes, buckyballs, ropes, and a universal graphitic potential. Physical Review B 62(19):13104-13310.

Gupta, S. S., Batra, R. C. (2008). Continuum structures equivalent in normal mode vibrations to single-walled carbon nanotubes. Computational Material Science 43:715-723.

Hayt, W. H., Buck, J. A. (2001). Engineering electromagnetics. 6th ed., McGrawHill (New York)

Jalili, N., Laxminarayana, K. (2004). A review of atomic force microscopy imaging systems: application to molecular metrology and biological sciences. Mechatronics 14(8):907-945.

Janghorban, M. (2011). Static and free vibration analysis of carbon nano wires based on Timoshenko beam theory using differential quadrature method. Latin American Journal of Solids and Structures 8: 463-472.

Ke, C. H., Pugno, N., Peng, B., Espinosa, H. D. (2005). Experiments and modeling of carbon nanotube-based NEMS devices. Journal of Mechanics and Physics of Solids 53**:**1314-1333.

Kim, P., Lieber, C. M. (1999). Nanotube nanotweezers. Science 286: 2148-2150.

Koochi, A., Kazemi, A. S., Tadi Beni, Y., Yekrangi, A., Abadyan, M. (2010) Theoretical study of the effect of Casimir attraction on the pull-in behavior of beam-type NEMS using modified Adomian method. Physica E 43(2):625-632.

Koochi, A., Noghrehabadi, A., Abadyan, M., Roohi, E. (2011a). Investigation of the effect of van der Waals force on the instability of electrostatic Nano-actuators, International Journal of Modern Physics B 25(29):3965–3976.

Koochi, A. Kazemi, A. S., Abadyan, M. (2011b). Simulating deflection and determining stable length of freestanding CNT probe/sensor in the vicinity of grapheme layers using a nano-scale continuum model. NANO 6(5): 419–429.

Koochi, A., Kazemi, A. S., Abadyan, M. (2012) Influence of Surface Effect on Size-Dependent Instability of Nano-Actuator in Presence of Casimir Force Physica Scripta 85:035804 (7pp).

Koochi, A. Abadyan, M., Hosseini-Toudeshky, H., Ovesy, H. R. (2013). Modeling the Influence of Surface Effect on Instability of nano-cantilever in Presence of van der Waals Force. Accepted for publish in International Journal for Structural Stability and Dynamics.

Lee SW. and Sigmund WM. (2002). "AFM study of repulsive Van der Waals forces between Teflon AF thin film and silica or alumina." Colloids and Surfaces A: Physicochemical and Engineering Aspects. 204 1-3, 43–50

Lennard-Jones, J. E. (1930).Perturbation Problems in Quantum Mechanics.Proceedig of the Royal Society A 129:598-615.

Li, C., Thostenson, E. T., Chou, T. W. (2008). Sensors and actuators based on carbon nanotubes and their composites: A review. Composites Science and Technology 68:1227–1249.

Lin WH, Zhao YP. (2003). Dynamics behavior of nanoscale electrostatic actuators. Chinese Physics Letters, 20: 2070-2073

Lin, W. H., Zhao, Y. P. (2005a). Casimir effect on the pull-in parameters of nanometer switches. Microsystem Technologies 11:80-85.

Lin, W. H., Zhao, Y. P. (2005b). Nonlinear behavior for nanoscale electrostatic actuators with Casimir force. Chaos Solitons and Fractals 23:1777–1785.

Moghimi Zand M., Ahmadian M.T. (2009). Application of homotopy analysis method in studying dynamic pull-in instability of microsystems. Mech. Research Communications 36:851-858.

Nayfeh, A. H., Younis, M. I., Abdel-Rahman, E. M. (2005) Reduced-order models for MEMS applications. Nonlinear Dynamics 41:211–236.

Noghrehabadi A., Ghalambaz M., Beni Y. T., Abadyan M., Abadi M. N., Abadi M. N. (2011). A new solution on the buckling and stable length of multi wall carbon nanotube probes near graphite sheets. Procedia Engineering 10:3725–3733.

Noghrehabadi A., Ghalambaz M., Ghanbarzadeh A. (2012). Buckling of multi wall carbon nanotube cantilevers in the vicinity of graphite sheets using mono- tone positive method. Journal of Computational and Applied Research in Mechanical Engineering 1:89–97.

Paradise, M., Goswami T. (2007). Carbon nanotubes–Production and industrial applications. Materials & Design 28(5):1477-1489.

Rach, R. (1984).A convenient computational form for the Adomian polynomials. Journal of Mathematical Analysis and Applications 102:415-419.

Rach, R. (2012). A bibliography of the theory and applications of the Adomian decomposition method, 1961-2011. Kybernetes 41(7,8):1087-1148.

Rasekh, M., Khadem, S. E. (2011). Pull-in analysis of an electrostatically actuated nano-cantilever beam with nonlinearity in curvature and inertia. International Journal of Mechanical Sciences 53:108–115.

Sedighi, H.M. (2014). Size-dependent dynamic pull-in instability of vibrating electrically actuated micro-beams based on the strain gradient elasticity theory. Acta Astronautica (in press).

Snow, E. S., Campbell, P. M., Novak, J. P. (2002a). Atomic force microscopy using single-wall C nanotube probes. Journal of Vacuum Science and Technology: B 20(3):822-827.

Snow, E. S., Campbell, P. M., Novak, J. P. (2002b). Single-wall carbon nanotube atomic force microscope probes. Applied Physics Letters 80(11):2002-2005.

Soroush, R., Koochi, A., Kazemi, A. S., Abadyan, M. (2012) Modeling the effect of van der Waals attraction on the instability of electrostatic Cantilever and Doubly-supported Nano-beams using Modified Adomian Method. International Journal for Structural Stability and Dynamics 12(5):1250036 (18 pp).

Tsai, J. L., Tu, J. F. (2010). Characterizing mechanical properties of graphite using molecular dynamics simulation. Materials and Design 31(1):194-199.

Tserpes, K. I. (2007). Role of intertube spacing in the pullout forces of double-walled carbon nanotubes. Materials & Design 28(7):2197-2201.

Wang, G. W., Zhang, Y., Zhao, Y. P., Yang, G. T. (2004).Pull-in stability study of nanotubes under van der Waals forces influence. Journal of Micromechanics and Microengineering 14: 1119-1125

Wazwaz, A. M. (2001). The numerical solution of sixth-order boundary value problems by the modified decomposition method. Applied Mathematics and Computation118:311-325.